Original Article

Disrupted rich club organization and structural brain connectome in unmedicated bipolar disorder

Ying Wang[1,2,*], Feng Deng[3,*], Yanbin Jia[4], Junjing Wang[3], Shuming Zhong[4], Huiyuan Huang[3], Lixiang Chen[3], Guanmao Chen[1], Huiqing Hu[3], Li Huang[1,2] and Ruiwang Huang[3]

[1]Medical Imaging Center, First Affiliated Hospital of Jinan University, Guangzhou 510630, China; [2]Institute of Molecular and Functional Imaging, Jinan University, Guangzhou 510630, China; [3]Center for the Study of Applied Psychology & MRI Center, Key Laboratory of Mental Health and Cognitive Science of Guangdong Province, School of Psychology, Institute for Brain Research and Rehabilitation, South China Normal University, Guangzhou 510631, China and [4]Department of Psychiatry, First Affiliated Hospital of Jinan University, Guangzhou 510630, China

Abstract

Background. Bipolar disorder (BD) has been associated with altered brain structural and functional connectivity. However, little is known regarding alterations of the structural brain connectome in BD. The present study aimed to use diffusion-tensor imaging (DTI) and graph theory approaches to investigate the rich club organization and white matter structural connectome in BD.

Methods. Forty-two patients with unmedicated BD depression and 59 age-, sex- and handedness-matched healthy control participants underwent DTI. The whole-brain structural connectome was constructed by a deterministic fiber tracking approach. Graph theory analysis was used to examine the group-specific global and nodal topological properties, and rich club organizations, and then nonparametric permutation tests were used for group comparisons of network parameters.

Results. Compared with healthy control participants, the patients with BD showed abnormal global properties, including increased characteristic path length, and decreased global efficiency and local efficiency. Locally, the patients with BD showed abnormal nodal parameters (nodal strength, nodal efficiency, and nodal betweenness) predominantly in the parietal, orbitofrontal, occipital, and cerebellar regions. Moreover, the patients with BD showed decreased rich club and feeder connectivity density.

Conclusions. Our results may reflect the disrupted white matter topological organization in the whole-brain, and abnormal regional connectivity supporting cognitive and affective functioning in depressed BD, which, in part, be due to impaired rich club connectivity.

Significant outcomes

- The patients with BD showed disrupted whole structural topological organization and rich club connections.
- The patients with BD showed abnormal nodal parameters predominantly in regions of the default mode network and central executive network.

Introduction

Bipolar disorder (BD) is a severe chronic mood disorder characterized by episodes of mania, hypomania, and alternating or intertwining episodes of depression (Grande *et al.*, 2016). The increasing body of multimodal neuroimaging evidence has shown structural and functional brain abnormalities in BD, mainly in the prefrontal cortex, temporal cortex, limbic system, and subcortical structures (Vargas *et al.*, 2013; Hanford *et al.*, 2016; Wise *et al.*, 2016). A recent major step forward in the field has been the realization that altered structural and functional connectivity between these regions is likely as crucial to the pathogenesis of BD as isolated changes in volume and functional activity (Calhoun *et al.*, 2011; O'Donoghue *et al.*, 2015; Wise *et al.*, 2016; O'Donoghue *et al.*, 2017a).

Diffusion-tensor imaging (DTI), the only available technique to study the microstructure of human brain white matter (WM) *in vivo*, has been used to detect WM abnormalities in patients with mood disorders (Sexton *et al.*, 2009). Previous DTI studies have demonstrated both local and widespread fractional anisotropy (FA) reductions in the brain WM regions in BD patients compared with healthy controls, such as in the corpus callosum, anterior limb of internal capsule, temporal-parietal WM, anterior and posterior cingulum (Vederine

CAMBRIDGE
UNIVERSITY PRESS

et al., 2011; O'Donoghue et al., 2017a), and these abnormalities have been attributed to disruptions in connectivity. A recent meta-analysis of DTI studies indicated that BD is most commonly associated with a WM disruption in the fronto-limbic connectivity, which may be accompanied by other WM changes spread throughout temporal and parietal regions (Bellani et al., 2016). However, the majority of DTI studies in BD are limited by small subject numbers and confounded by the use of psychotropic medications (i.e. lithium, mood stabilizers, antipsychotics, and antidepressant medication) (Hafeman et al., 2012). In general, the literature to date supports a normalizing effect of lithium and mood stabilizers on brain structure in BD, which is consistent with the neuroprotective characteristics of these medications identified by preclinical studies (Fisher et al., 2015). In addition, most studies involve heterogeneous samples of BD patients combining subjects in different mood states (i.e. manic, depressive, euthymic, and mixed states), which could have different neural network activation correlates and different WM DTI patterns (Zanetti et al., 2009; Bellani et al., 2016; Serpa et al., 2017). Therefore, to better understand the brain structural changes in BD patients, the aforementioned limitations need to be overcome in research.

Rather than investigating individual regions or tracts in isolation, the brain can be analyzed as a complex and integrative network known as the human connectome (Sporns, 2011). A graph theoretical framework enables the study of a large-scale brain structural network by characterizing the brain regions as nodes and the WM tracts as edges (Sporns et al., 2005; Puetz et al., 2017). Network studies of structural connectivity obtained from DTI have revealed that healthy human WM networks exhibit 'small-world' networks that have an optimal balance between local specialization and global integration for information processing (Sporns, 2011). In addition, network hubs form a high capacity central core, or rich club, and rich club connections play a key role in promoting global communication and information integration (van den Heuvel and Sporns, 2011; Liang et al., 2017). Several studies have found disrupted small-world properties and abnormal regional characteristics in various neurological and psychiatric disorders, including Alzheimer's disease (Shu et al., 2012), major depression disorder (Bai et al., 2012; Korgaonkar et al., 2014), and schizophrenia (van den Heuvel et al., 2013; Griffa et al., 2015). Moreover, many connectivity studies hypothesized either that these diseases may target certain connections in the rich club network (Shu et al., 2012; van den Heuvel et al., 2013), or that network disruptions in the rich club have the most significant impact on cognition (Daianu et al., 2016). Until now, few studies have found changed whole-brain structural network in BD (Leow et al., 2013; Collin et al., 2016; O'Donoghue et al., 2017b), and those studies that did were inconsistent in the network topological properties that they reported. A number of confounding factors might influence structural network results and, thus, could at least partly account for this heterogeneity, including medication status, mood status, age range, chronicity, and long duration of illness.

In this study, we use DTI and graph theory approaches to investigate the rich club organization and structural brain connectome in unmedicated patients with BD depression. On the basis of previous findings in the functional and structural connectome (Leow et al., 2013; Wang et al., 2017a), we hypothesized that in BD the structural connectome would show disrupted whole topological organization and rich club connections, and abnormal regional connectivity supporting cognitive and affective functioning.

Materials and methods

Participant

This prospective study was approved by the Ethics Committee of First Affiliated Hospital of Jinan University (Guangzhou, China), the written informed consent of each participant was obtained before the study. Patients were recruited from January 2015 to January 2017. In total, 42 right-handed, nonsmokers, out- or in-patients with BD were recruited from the psychiatry department of First Affiliated Hospital of Jinan University, Guangzhou, China. The patients were aged from 18 to 55 years. All patients met DSM-IV (Diagnostic and Statistical Manual of Mental Disorders, Fourth Edition) criteria for BD according to the diagnostic assessment by the Structured Clinical Interview for DSM-IV Patient Edition. Diagnosis of BD was determined by two experienced clinical psychiatrists. Among the 42 BD patients, seven were diagnosed with BD-I type and 35 with BD-II type. Exclusion criteria included the presence of (a) any current psychiatric disorder (with the exception of BD and anxiety disorders); (b) a history of electroconvulsive therapy; (c) any history of moderate/severe head injury, head trauma, neurological disorder, or mental retardation; (d) alcohol/substance abuse or dependence; and (e) the presence of a concurrent significant physical illness. No patients were excluded for the exclusion criteria. The clinical state was assessed using the 24-item Hamilton Depression Rating Scale (HDRS) and the Young Mania Rating Scale (YMRS) during the 3-day period prior to the imaging session. All patients with BD were suffering from depression (HDRS-24 score ⩾21, YMRS score <7). At the time of the scanning, all patients were either medication-naïve or were unmedicated for at least 6 months. Among them, 11 patients were medication-naïve; they had never been diagnosed or did not want to take medication. While for the others, the recruited patients generally visited their physicians (psychiatrist/general practitioner) because of depressive relapse after quitting the medication. These 31 patients had been treated with antidepressants (duloxetine or paroxetine), and/or mood stabilizers (lithium, sodium valproate), and/or atypical antipsychotic medications (olanzapine or risperidone), but had been off medication for at least 6 months prior to the scan.

A total of 59 right-handed, nonsmokers healthy control participants matched for sex and age were recruited via local advertisements. All healthy control participants were interviewed to rule out the presence of current or past psychiatric illness. Further exclusion criteria for healthy controls were any history of psychiatric illness in first-degree relatives, current or past significant medical or neurological illness.

MRI data acquisition and preprocessing

All MRI data were acquired on a 3.0 T MR system (Discovery MR 750 System, GE Healthcare, Milwaukee, WI) with an eight-channel phased-array head coil. The DTI data were obtained using a single-shot spin-echo diffusion-weighted EPI sequence with the following parameters: repetition time ms/echo time ms, 8000/68; flip angle, 90°; field of view, 256×256 mm^2; 128×128 matrix; 30 different diffusion directions with $b = 1000$ s/mm^2, five non-diffusion weighted b_0 volumes, slice thickness, 2 mm; no intersection gap, and 75 interleaved axial slices covering the whole brain. For each subject, the DTI scan was performed twice, and the two DTI datasets were subsequently averaged to increase the signal-to-noise ratio (SNR). A three-

dimensional brain volume imaging sequence that covered the whole brain was used for structural data acquisition (8.2/3.2; flip angle, 12°; field of view, 240 × 240 mm^2; 256 × 256 matrix, slice thickness = 1 mm; no intersection gap). In addition, two routine scans using axial T$_1$-weighted fluid attenuation inversion recovery and fast spin echo T$_2$-weighted MR sequences were also applied to obtain brain images to confirm the absence of any brain structural abnormalities. All MR images were evaluated by two neuroradiologists.

DTI data preprocessing and network construction

All DTI data were processed with PANDA package (Cui *et al.*, 2013) under a Linux Operating System. For each subject, the two DTI datasets were concatenated together and the effects of head motion and image distortions caused by eddy-currents were corrected using FSL/FDT (http://www.fmrib.ox.ac.uk/fsl). In detail, the ten b_0 images (two scans) were extracted and aligned to the first b_0 image. Then we averaged the ten b_0 images and affine alignment of each of 60 diffusion-weighted image volumes (two scans) to the averaged b_0 images was applied. Diffusion-sensitive gradients were adjusted to account for the rotation applied to the measurements during motion correction (Leow *et al.*, 2013). Afterward, the 60 diffusion-weighted image volumes were split into two DTI datasets (30 volumes for each dataset), which were averaged and merged with the averaged b_0 images. Then we estimated voxel-wise diffusion tensor and obtained the FA maps.

We took revised automated anatomical labeling v2 (AAL2) atlas (Rolls *et al.*, 2015), which parcellates the whole brain into 120 cortical and subcortical regions of interest (ROIs), as a node and the inter-nodal WM streamlines as the edge to construct the network for each subject. The names and abbreviations of these ROIs are presented in the online Supplementary Table S1. In specific, each of the FA maps in native space was affinely coregistered to its corresponding T$_1$-weigted images. Then, T$_1$-weighted images were nonlinearly registered to the MNI space. The inverse transformations were obtained to the above two steps to transform the AAL2 atlas from MNI space to diffusion native space. Each ROI from AAL2 atlas represents a node of a structural brain network. A whole brain deterministic tractography approach was performed using the fiber assignment by continuous tracking (FACT) algorithm (Mori and Zijl, 2002). In the calculations, fiber tracking was terminated at voxels where FA < 0.2 or where the angle between two eigenvectors to be connected by the tracking was greater than 45°. We took the mean FA value along the inter-regional streamlines as the edge weight and constructed an FA-weighted 120 × 120 matrix for each subject. To reduce the potential effect of noise or other factors during diffusion tractography caused by data acquisition and pre-/post-processing, we considered two ROIs were structurally connected if at least three streamlines connecting them (Lo *et al.*, 2010; Shu *et al.*, 2011). Such a threshold selection reduced the risk of false-positive connections due to noise or the limitations in the deterministic tractography and simultaneously ensured the size of the largest connected component in the prospective network.

Graph analysis of network topology

Global and nodal parameters

All network analyses were performed using GRETNA (http://www.nitrc.org/projects/gretna/) and illustrated using BrainNet

Viewer (http://www.nitrc.org/projects/bnv/). We characterized the global properties of brain structural networks by the following parameters: characteristic path length (L_p), clustering coefficient (C_p), global efficiency (E_{glob}), local efficiency (E_{loc}), normalized clustering coefficient (γ), and normalized characteristic path length (λ) (Rubinov and Sporns, 2009). Typically, a small-world network is characterized as $\gamma \gg 1$ and $\lambda \approx 1$, or $\delta = \gamma/\lambda > 1$ (Taira *et al.*, 2014). In other words, a small-world network has not only the higher local interconnectivity but also the approximately equivalent shortest path length compared with the random networks (Cao *et al.*, 2013). Three nodal parameters characterizing nodal properties of brain structural networks were also calculated: nodal strength (K_i), nodal efficiency (E_i), and nodal betweenness (B_i). The definitions and interpretations of these global and nodal parameters are listed in the online Supplementary Table S2.

Rich club analysis

The rich club organization described central backbone for global communication in the brain network (van den Heuvel and Sporns, 2011; van den Heuvel *et al.*, 2012), refers to nodes with higher degrees within brain networks and a higher connectivity strength of inter-nodal connections (van den Heuvel and Sporns, 2011). In the present study, the group-averaged FA-weighted structural networks were constructed for the BD and the control groups separately. The weighted rich club coefficient $\phi^w(k)$, randomly rich club coefficient $\phi^w_{rand}(k)$, and normalized rich club coefficient $\phi^w_{norm}(k)$ for each group were calculated to describe rich club organization, the details of which are given in the Supplemental Material. The rich club regions were selected at the top 12% of most consistently ranked nodes across two groups (van den Heuvel *et al.*, 2013). Three classes of connections were used to characterize the edge architecture of brain networks as follows: rich club connections which link rich club nodes to rich club nodes, feeder connections which link rich club nodes to non-rich club nodes, and local connections which link non-rich club nodes to non-rich club nodes.

Statistical analysis

Comparison of demographic variables

We applied χ^2-test to determine the gender difference and independent two sample *t* test (two-tailed) to determine the age and education difference between the BD and the control groups.

Comparison of network parameters

A non-parametric permutation test (10 000 times) was used to determine the statistical significance of between-group differences in network parameters (global and nodal parameters, rich club coefficient, feeder, and local connectivity density). Non-parametric methods use the data itself to find the null distribution, allowing the consideration of non-standard test statistics (Poldrack *et al.*, 2011). Under the null hypothesis, the group labels are irrelevant, and thus we can reanalyze the data over and over with different permutations of the labels. To correct the multiple comparisons for nodal parameters, false positive correction for N-node statistical comparison was applied using 1/(amount of nodes) = 1/120 = 0.0083 as significance threshold (Bassett *et al.*, 2009; Meng *et al.*, 2014), which is equivalent to saying that nodes with $p < 0.0083$ to be 'significant'. Although this correction method is not as conservative as a Bonferroni or FDR correction, it has been used in many studies, particularly for comparisons of regional network

metrics (Lynall *et al.*, 2010; Jung *et al.*, 2017). When we compared group differences of those network parameters (global and nodal parameters as well as rich club organizations), we took age, gender, and education levels as nuisance covariates and regressed them out.

Relationship between network parameters and clinical variables

For the network parameters that showed significant between-group differences, we computed partial correlations between these parameters and clinical variables for the BD patients (i.e. HDRS scores, number of episodes, durations of illness, and onset age of illness) controlling for age, gender, and education levels ($p < 0.05$, FDR-corrected).

Results

Demographic and clinical variables

Table 1 shows the demographic and clinical data of all study participants. There were no significant differences in sex and age between the BD group and the healthy control group ($p > 0.05$). The control group received a significantly higher level of education than the BD group (two-tailed *t* test, $p < 0.001$).

Network analyses

Global and nodal parameters

Figure 1 shows the global parameters of brain networks in the BD and the control groups. The small-world properties of structural networks were estimated for the BD patients and the controls. We found $\delta > 1$ for both groups, which suggest that the structural networks of both subject groups possess small-world characteristics. In addition, we found increased L_p ($p = 0.037$), and decreased E_{glob} ($p = 0.043$) and E_{loc} ($p = 0.021$) in the BD group compared with the controls.

Figure 2 and Table 2 show the differences in nodal parameters of brain networks in the BD group compared with the controls. The BD group exhibited significantly decreased K_i compared with the controls in three regions, the left cuneus (CUN.L, $p = 0.006$), right cerebelum_7b (HVIIb.R, $p = 0.002$), and right cerebelum_Crus2 (Hcrus II.R, $p = 0.001$). And compared with

the controls, the BD group showed significantly decreased E_i in two regions: the left superior parietal gyrus (SPG.L, $p = 0.001$) and left angular gyrus (ANG.L, $p = 0.004$). In addition, we also found that the BD group showed significantly increased B_i in the left orbital part of inferior frontal gyrus (IFGorb.L, $p = 0.003$), and right calcarine gyrus (CAL.R, $p = 0.003$) compared with the controls.

Rich club analysis

Figure 3*a* illustrates the rich club organization found in the structural networks of both the BD and control groups. For the BD and control groups, we found the normalized rich club coefficients $\phi^w_{norm}(k) > 1$ over the range of degrees from $k = 1$–16 (Fig. 3*a*). However, no significant differences were detected in normalized rich club coefficients $\phi^w_{norm}(k)$ between the BD and the control groups (Fig. 1*a*). We detected 14 rich club regions, which are located in the bilateral medial superior frontal gyrus (SFGmedial), superior frontal gyrus (SFG), calcarine (CAL), cuneus (CUN), precuneus (PCUN), putamen (PUT), and superior parietal gyrus (SPG) (Fig. 3*b*).

When characterizing the edge architecture in the context of rich club organization, we found both the rich club ($p = 0.03$) and feeder connections ($p = 0.04$) were decreased in the BD group compared with the controls (permutation testing, 10 000 times, Fig. 3*c*). That is, the connections that link the group-averaged rich club regions and the connections that link the group-averaged rich club regions with non-rich club regions. No significant group effect was found in the local connections ($p = 0.08$), which connect the non-rich club regions.

Relationship between network parameters and clinical variables

For the correlations between network parameters and clinical variables, no significant correlation results survived after FDR correction ($p < 0.05$, FDR-corrected). We have also displayed the correlation results without correction in the online Supplementary Fig. S1.

Discussion

Using DTI tractography, this study detected abnormal topological organization of WM networks in homogeneous unmedicated adult patients with depressed BD. We found that compared with the healthy controls, the BD patients showed (1) increased L_p, and decreased E_{glob} and E_{loc}; (2) abnormal nodal parameters mainly in the parietal, orbitofrontal, occipital, and cerebellar regions; (3) decreased rich club connectivity density and feeder connectivity density. These findings extend our understanding of the neuropathological mechanisms underlying BD from a perspective of WM structural connectivity pattern.

In this study, we found altered global topological properties of the whole brain structural networks in the unmedicated patients with depressed BD, including increased L_p, and decreased E_{glob} and E_{loc}, which suggests a less optimized topological organization in their WM networks. These findings were partly consistent with the BD-related brain networks studies using DTI (Leow *et al.*, 2013; Collin *et al.*, 2016; O'Donoghue *et al.*, 2017*b*), resting state fMRI (Spielberg *et al.*, 2016; Wang *et al.*, 2017*a*), and EEG (Kim *et al.*, 2013). For example, two structural brain network studies found that medicated patients with euthymic BD I exhibited longer L_p, lower E_{glob}, and lower C_p than controls, suggesting

Table 1. Demographic and clinical data in patients with BD and healthy control group

|	BD	control	*p* value
No. of participants	42	59	
Age (years)	25.95 ± 7.93	27.51 ± 8.40	0.35[a]
Gender (male/female)	28M/14F	31M/28F	0.16[b]
Education (years)	13.52 ± 3.23	15.97 ± 2.34	0.00[a]
HRSD-24 score (points)	27.21 ± 6.66	–	
YMRS score (points)	3.90 ± 5.63	–	
Number of episodes	2.88 ± 1.63	–	
Age of onset (years)	21.64 ± 9.70	–	
Disease of illness (months)	46.61 ± 61.48	–	

HRSD-24, the 24-item Hamilton Rating Scale; YMRS, Young Mania Rating Scale.
[a]*p* value obtained using the two-tailed two sample *t* test.
[b]*p* value obtained using the χ^2 test.
Means ± standard deviations are reported unless otherwise noted.
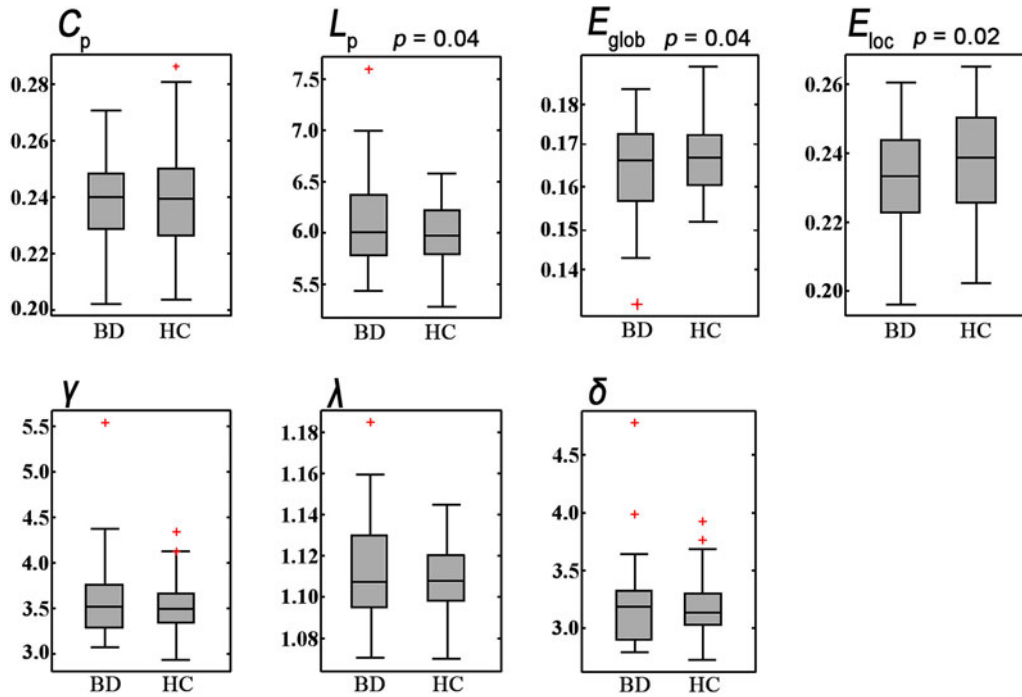
Fig. 1. The differences in global parameters of the brain anatomical networks between the bipolar disorder (BD) patients and the controls (HC). The BD patients showed significant decreases in E_{glob}, and E_{loc}, but significant increases in L_p compared with the controls ($p < 0.05$, permutation test). The symbol of '+' in red color indicates outliers. Abbreviations: C_p, clustering coefficient; L_p, shortest path length; E_{glob}, global efficiency; E_{loc}, local efficiency; λ, normalized characteristic path length; γ, normalized clustering coefficient; $\delta = \lambda/\gamma$, small-world characteristic.

impaired global integration in BD patients (Leow *et al.*, 2013; O'Donoghue *et al.*, 2017*b*). In addition, previous studies using DTI tractography and graph theory approaches proposed the disease-related increases in the L_p may be attributable to the degeneration of fiber bundles used for information transmission

(Bai *et al.*, 2012). Taken together, our findings of abnormal global topological properties in depressed BD suggest a disturbance between segregation and integration in brain structural networks, which could indicate distributed information transmission in BD.
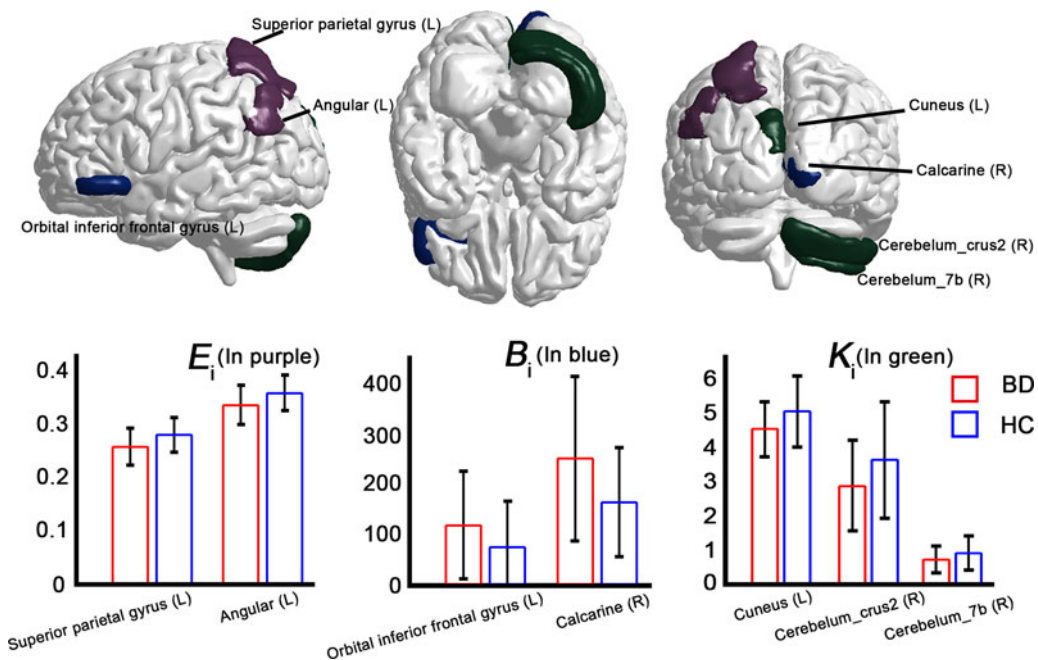

Fig. 2. Brain regions with significantly changed nodal parameters in the bipolar disorder (BD) patients. The BD patients showed significantly decreased nodal degree (K_i), represented by green color, and nodal efficiency (E_i), represented by purple color, in five regions and significantly increased nodal betweenness (B_i), represented by blue color, in two regions compared with the healthy controls (HC).

Table 2. Brain regions showing altered nodal parameters (nodal degree K_i, nodal efficiency E_i, and nodal betweenness B_i) of brain structural networks in the BD patients compared with the healthy controls (HC)

Parameters	Regions	Group	Mean (s.d.)	p value
K_i	Left cuneus	BD	4.54 (0.80)	6.30E-03
		HC	5.06 (1.06)	
	Right cerebelum_crus2	BD	2.86 (1.33)	1.10E-03
		HC	3.63 (1.71)	
	Right cerebelum_7b	BD	0.69 (0.37)	2.40E-03
		HC	0.88 (0.50)	
E_i	Left parietal_sup	BD	0.26 (0.03)	9.00E-04
		HC	0.28 (0.03)	
	Left angular	BD	0.33 (0.04)	4.20E-03
		HC	0.36 (0.03)	
B_i	Left frontal_inf_orb_2	BD	117 (107)	3.40E-03
		HC	73.7 (93.3)	
	Right calcarine	BD	252 (165)	3.30E-03
		HC	164 (111)	

Turning to the nodal level, we found altered nodal parameters (K_i, E_i, or B_i) in the depressed BD patients mainly in regions of the default mode network (DMN) including the angular gyrus and cuneus, and regions of the central executive network (CEN, also referred to as the cognitive control network) including the SPG, orbital part of inferior frontal gyrus, and posterior cerebellum. This suggested disconnections of the WM in these regions

in BD patients. The DMN is believed involving in affective regulation and internal thoughts (Kaiser et al., 2015); and the CEN is responsible for high-level cognitive functions and external information procession (Menon, 2011). Previous fMRI studies have reported impairments in the coordinated activity, functional connectivity within and between the DMN and CEN in BD patients (Goya-Maldonado et al., 2016; Wang et al., 2016), which might be
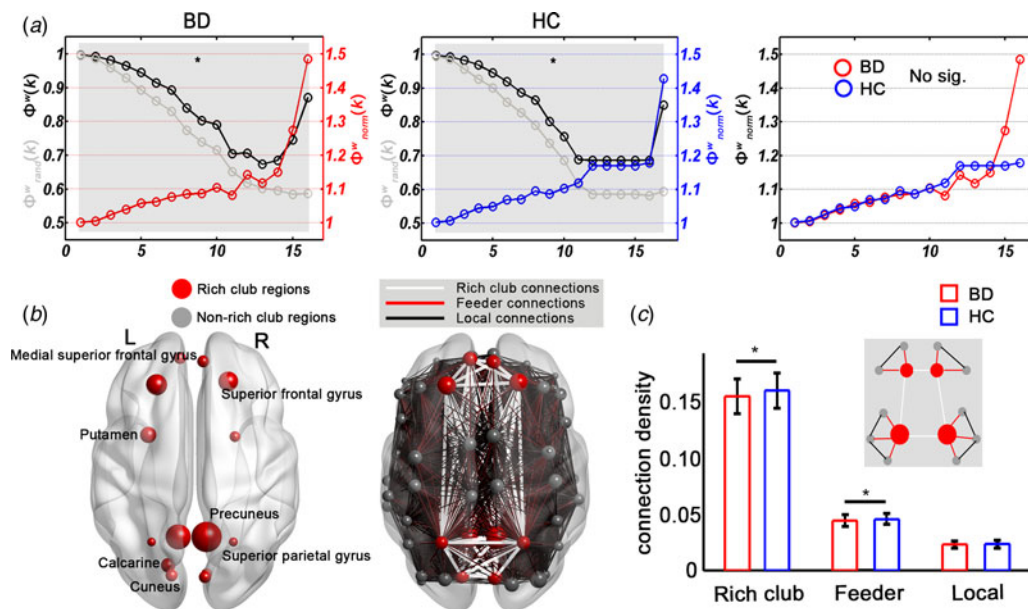
Fig. 3. Comparison of group-averaged rich club organization between the bipolar disorder (BD) patients and the healthy controls (HC). (a) Normalized rich club coefficient $\phi_{norm}^{w}(k)$ original rich club coefficient $\phi^{w}(k)$ and the randomly rich club coefficient $\phi_{rand}^{w}(k)$. Each symbol 'o' in red (blue) indicates the normalized rich club coefficient for the patients (controls) at specific degree k. The gray area indicates $\phi_{norm}^{w}(k) >1$ for each group. The patient group did not show a significant difference in rich club organization compared with controls. (b) Rich club members included the bilateral medial superior frontal gyrus, superior frontal gyrus, calcarine, cuneus, precuneus, putamen, and superior parietal gyrus in both healthy and patient populations. (c) Edges across individual brain networks (both controls and patients) were divided into three distinct classes: rich club connections linking rich club members (white), feeder connections linking rich club members to non-rich club members (red), and local connections connecting non-rich club members (black).

related to cognitive impairments and clinical symptoms. For example, the functional imbalance between the DMN and CEN is correlated with depressive symptoms or trait rumination and is not present during a self-focus condition, suggesting a failure to reallocate resources away from self-referential processing toward external goal-directed behavior when this is required (Belleau *et al.*, 2015; Kaiser *et al.*, 2015; Lois *et al.*, 2017). Our findings, combined with these previous reports, suggest that disrupted WM connectivity in the DMN and CEN regions may contribute to core deficits in cognitive and affective functioning in depressed BD. Unfortunately, we failed to observe the correlation between altered nodal parameters and clinical variables. In addition, several fMRI studies found impaired DMN in euthymic BD and their unaffected siblings (Alonso-Lana *et al.*, 2016; Lois *et al.*, 2017; Wang *et al.*, 2017*b*), and suggested that it may act as a trait marker. Therefore, the present findings need confirmation in further studies combining DTI and fMRI measurement in BD across different mood phases, preferably with a longitudinal, within-subject design.

The rich club organization takes a central position in the brain's network topology, and connections among rich club brain hubs have been proposed to be central to the integration of information among different subsystems of the human brain (van den Heuvel and Sporns, 2011; van den Heuvel *et al.*, 2013). In this study, we detected decreased rich club connectivity density and feeder connectivity density in the BD patients. This may suggest that the rich club connections among the central hubs, acted as a central high cost and high capacity backbone for global brain communication (van den Heuvel *et al.*, 2012), were prone to be disrupted in BD patients. Several structural network studies found reduced rich club connectivity in schizophrenia patients (van den Heuvel *et al.*, 2013; Collin *et al.*, 2014; Klauser *et al.*, 2017) and their unaffected siblings (Collin *et al.*, 2014), indicating a disproportionate disturbance of brain hubs and their mutual connections in schizophrenia. However, a recent DTI study found no indication that the brain hubs or 'rich club' connections were particularly affected in BD patients (Collin *et al.*, 2016). It is worthy to note that, in their study, the majority of the BD patients were euthymic, and the patients used psychotropic medications including lithium and antipsychotics. In addition, the identified rich club regions or hubs in the present study comprised the precuneus, cuneus, superior frontal cortex, superior parietal cortex, calcarine, and putamen in the BD patients and controls, consistent with previous studies (van den Heuvel and Sporns, 2011; Collin *et al.*, 2014; Tuladhar *et al.*, 2017). Due to their central position in the topology of the network, the connections among these rich club nodes may play an important role in the efficient integration of information processing among distant brain regions (i.e. global efficiency of the network) (van den Heuvel and Sporns, 2011; van den Heuvel *et al.*, 2012). Damage specifically to the rich club connections seems to have a more severe impact on global efficiency than random damage to the network (van den Heuvel and Sporns, 2011). Therefore, these findings, in conjunction with the global parameters changes, suggest that the abnormal whole brain network organization in BD might, in part, be due to impaired rich club connections. Moreover, we found these altered nodal parameters specifically affecting rich club regions, such as the cuneus, calcarine, and superior parietal cortex, suggesting that specific core areas of the brain might be preferentially targeted by BD pathology.

This study has several limitations. First, the node and edge definitions and DTI acquisition protocols may affect the findings obtained from whole brain WM structural networks in BD patients. However, there is no widely agreed-on approach for calculating the brain network metrics. This suggests the measures may not be optimally robust just yet. In this study, we selected a widely applied template, the AAL-120 template, to define the network nodes. Regions on the AAL template differ in size, which may have a confounding effect on the link weight of the network nodes. Thus, we also used a high-resolution (∼1000 parcels) parcellation (AAL-1024) by randomly subdividing the AAL atlas into 1024 regions with equal size both in the volume and in the average cortical surface, and the results were similar to our main findings (online Supplementary Table S4). Deterministic fiber tractography was used to define the edges of the structural connectome, which may result in the loss of existing fibers due to the 'fiber crossing' problem. Tensor-based deterministic tractography approaches yield sparse connectomes and contain false negatives (high specificity with comparatively low sensitivity), whereas probabilistic methods steered by crossing-fiber models yield dense connectomes and contain false positives (high sensitivity with comparatively low specificity), other groups have begun to study tradeoffs between connectome sensitivity and specificity (Zalesky *et al.*, 2016). Initial studies in this regard suggest (both empirically and theoretically) that specificity is at least twice as important as sensitivity when estimating key properties of brain networks (Zalesky *et al.*, 2016). Second, the BD patients were recruited including BD type I and type II. There were some clinical and anatomical data showing the differences between the subtypes (Abe *et al.*, 2016). However, we also did the same network analysis in 35 patients with only BDII and controls, and the results were similar to our main findings (online Supplementary Tables S6 and S7). Third, a significant difference in education level existed between the BD patients and the healthy controls, which may confound the statistical results. In order to minimize this effect, we took the education level as a nuisance covariate and regressed them out in all analyses. Fourth, the correlation results between network metrics and clinical variables did not survive after FDR correction, perhaps because of our relatively small sample size. Fifth, without a group of patients with BD in a euthymic episode, it is still not clear whether disrupted topological organization are specific to the depression episode of BD or shared by all episodes of the disease. Further studies using a prospective design may clarify this issue.

In conclusion, our study revealed the disrupted WM topological organization in the whole-brain, and abnormal regional connectivity supporting cognitive and affective functioning in BD, which, in part, be due to impaired rich club connectivity. Further longitudinal research is needed to examine how and whether the changes of WM connectivity, including the investigation of the rich club properties, are related to clinical deterioration in BD patients.

Conflict of interest. All authors declare that they have no conflicts of interest.

References

Abe C *et al.* (2016) Cortical thickness, volume and surface area in patients with bipolar disorder types I and II. *Journal of Psychiatry Neuroscience* **41**, 240–250.

Alonso-Lana S *et al.* (2016) Brain functional changes in first-degree relatives of patients with bipolar disorder: evidence for default mode network dysfunction. *Psychological Medicine* **46**, 2513–2521.

Bai F *et al.* (2012) Topologically convergent and divergent structural connectivity patterns between patients with remitted geriatric depression and amnestic mild cognitive impairment. *Journal of Neuroscience* **32**, 4307–4318.

Bassett DS *et al.* (2009) Cognitive fitness of cost-efficient brain functional networks. *Proceedings of the National Academy of Sciences of the United States of America* **106**, 11747–11752.

Bellani M *et al.* (2016) DTI and myelin plasticity in bipolar disorder: integrating neuroimaging and neuropathological findings. *Frontiers in Psychiatry* **7**, 21.

Belleau EL, Taubitz LE and Larson CL (2015) Imbalance of default mode and regulatory networks during externally focused processing in depression. *Social Cognitive and Affective Neuroscience* **10**, 744–751.

Calhoun VD *et al.* (2011) Exploring the psychosis functional connectome: aberrant intrinsic networks in schizophrenia and bipolar disorder. *Frontiers in Psychiatry* **2**, 75.

Cao Q *et al.* (2013) Probabilistic diffusion tractography and graph theory analysis reveal abnormal white matter structural connectivity networks in drug-naive boys with attention deficit/hyperactivity disorder. *Journal of Neuroscience* **33**, 10676–10687.

Collin G *et al.* (2014) Impaired rich club connectivity in unaffected siblings of schizophrenia patients. *Schizophrenia Bulletin* **40**, 438–448.

Collin G *et al.* (2016) Brain network analysis reveals affected connectome structure in bipolar I disorder. *Human Brain Mapping* **37**, 122–134.

Cui Z *et al.* (2013) PANDA: a pipeline toolbox for analyzing brain diffusion images. *Frontiers in Human Neuroscience* **7**, 42.

Daianu M *et al.* (2016) Disrupted rich club network in behavioral variant frontotemporal dementia and early-onset Alzheimer's disease. *Human Brain Mapping* **37**, 868–883.

Fisher AC *et al.* (2015) Neurophysiological correlates of dysregulated emotional arousal in severe traumatic brain injury. *Clinical Neurophysiology* **126**, 314–324.

Goya-Maldonado R *et al.* (2016) Differentiating unipolar and bipolar depression by alterations in large-scale brain networks. *Human Brain Mapping* **37**, 808–818.

Grande I *et al.* (2016) Bipolar disorder. *Lancet* **387**, 1561–1572.

Griffa A *et al.* (2015) Characterizing the connectome in schizophrenia with diffusion spectrum imaging. *Human Brain Mapping* **36**, 354–366.

Hafeman DM *et al.* (2012) Effects of medication on neuroimaging findings in bipolar disorder: an updated review. *Bipolar Disorders* **14**, 375–410.

Hanford LC *et al.* (2016) Cortical thickness in bipolar disorder: a systematic review. *Bipolar Disorders* **18**, 4–18.

Jung WH *et al.* (2017) Altered functional network architecture in orbitofronto-striato-thalamic circuit of unmedicated patients with obsessive-compulsive disorder. *Human Brain Mapping* **38**, 109–119.

Kaiser RH *et al.* (2015) Large-scale network dysfunction in major depressive disorder: a meta-analysis of resting-state functional connectivity. *JAMA Psychiatry* **72**, 603–611.

Kim DJ *et al.* (2013) Disturbed resting state EEG synchronization in bipolar disorder: a graph-theoretic analysis. *NeuroImage: Clinical* **2**, 414–423.

Klauser P *et al.* (2017) White matter disruptions in schizophrenia Are spatially widespread and topologically converge on brain network hubs. *Schizophrenia Bulletin* **43**, 425–435.

Korgaonkar MS *et al.* (2014) Abnormal structural networks characterize major depressive disorder: a connectome analysis. *Biological Psychiatry* **76**, 567–574.

Leow A *et al.* (2013) Impaired inter-hemispheric integration in bipolar disorder revealed with brain network analyses. *Biological Psychiatry* **73**, 183–193.

Liang X *et al.* (2017) The rich-club organization in Rat functional brain network to balance between communication cost and efficiency. *Cerebral Cortex* **28**, 924–935.

Lo CY *et al.* (2010) Diffusion tensor tractography reveals abnormal topological organization in structural cortical networks in Alzheimer's disease. *Journal of Neuroscience* **30**, 16876–16885.

Lois G *et al.* (2017) Large-scale network functional interactions during distraction and reappraisal in remitted bipolar and unipolar patients. *Bipolar Disorders* **19**, 487–495.

Lynall ME *et al.* (2010) Functional connectivity and brain networks in schizophrenia. *Journal of Neuroscience* **30**, 9477–9487.

Meng C *et al.* (2014) Aberrant topology of striatum's connectivity is associated with the number of episodes in depression. *Brain* **137**, 598–609.

Menon V (2011) Large-scale brain networks and psychopathology: a unifying triple network model. *Trends in Cognitive Sciences* **15**, 483–506.

Mori S and Zijl P (2002) Fiber tracking: principles and strategies – a technical review. *NMR in Biomedicine* **15**, 468–480.

O'Donoghue S *et al.* (2015) Applying neuroimaging to detect neuroanatomical dysconnectivity in psychosis. *Epidemiology and Psychiatric Sciences* **24**, 298–302.

O'Donoghue S *et al.* (2017a) Anatomical dysconnectivity in bipolar disorder compared with schizophrenia: a selective review of structural network analyses using diffusion MRI. *Journal of Affective Disorders* **209**, 217–228.

O'Donoghue S *et al.* (2017b) Anatomical integration and rich-club connectivity in euthymic bipolar disorder. *Psychological Medicine* **47**, 1609–1623.

Poldrack RA, Mumford JA and Nichols TE (2011) *Handbook of Functional MRI Data Analysis.* New York, NY: Cambridge University Press.

Puetz VB *et al.* (2017) Altered brain network integrity after childhood maltreatment: a structural connectomic DTI-study. *Human Brain Mapping* **38**, 855–868.

Rolls ET, Joliot M and Tzourio-Mazoyer N (2015) Implementation of a new parcellation of the orbitofrontal cortex in the automated anatomical labeling atlas. *Neuroimage* **122**, 1–5.

Rubinov M and Sporns O (2009) Complex network measures of brain connectivity: uses and interpretations. *Neuroimage* **52**, 1059–1069.

Serpa MH *et al.* (2017) State-dependent microstructural white matter changes in drug-naive patients with first-episode psychosis. *Psychological Medicine* **47**, 2613–2627.

Sexton CE, Mackay CE and Ebmeier KP (2009) A systematic review of diffusion tensor imaging studies in affective disorders. *Biological Psychiatry* **66**, 814–823.

Shu N *et al.* (2011) Diffusion tensor tractography reveals disrupted topological efficiency in white matter structural networks in multiple sclerosis. *Cerebral Cortex* **21**, 2565–2577.

Shu N *et al.* (2012) Disrupted topological organization in white matter structural networks in amnestic mild cognitive impairment: relationship to subtype. *Radiology* **265**, 518–527.

Spielberg JM *et al.* (2016) Resting state brain network disturbances related to hypomania and depression in medication-free bipolar disorder. *Neuropsychopharmacology* **41**, 3016–3024.

Sporns O (2011) The human connectome: a complex network. *Annals of the New York Academy of Sciences* **1224**, 109–125.

Sporns O, Tononi G and Kotter R (2005) The human connectome: a structural description of the human brain. *PLoS Computational Biology* **1**, e42.

Taira U *et al.* (2014) Efficiency of a 'small-world' brain network depends on consciousness level: a resting-state FMRI study. *Cerebral Cortex* **24**, 1529–1539.

Tuladhar AM *et al.* (2017) Disruption of rich club organisation in cerebral small vessel disease. *Human Brain Mapping* **38**, 1751–1766.

van den Heuvel MP and Sporns O (2011) Rich-club organization of the human connectome. *Journal of Neuroscience* **31**, 15775–15786.

van den Heuvel MP *et al.* (2012) High-cost, high-capacity backbone for global brain communication. *Proceedings of the National Academy of Sciences of the United States of America* **109**, 11372–11377.

van den Heuvel MP *et al.* (2013) Abnormal rich club organization and functional brain dynamics in schizophrenia. *JAMA Psychiatry* **70**, 783–792.

Vargas C, Lopez-Jaramillo C and Vieta E (2013) A systematic literature review of resting state network–functional MRI in bipolar disorder. *Journal of Affective Disorders* **150**, 727–735.

Vederine FE *et al.* (2011) A meta-analysis of whole-brain diffusion tensor imaging studies in bipolar disorder. *Progress in Neuro-Psychopharmacology & Biological Psychiatry* **35**, 1820–1826.

Wang Y *et al.* (2016) Disrupted resting-state functional connectivity in non-medicated bipolar disorder. *Radiology* **280**, 529–536.

Wang Y *et al.* (2017*a*) Topologically convergent and divergent functional connectivity patterns in unmedicated unipolar depression and bipolar disorder. *Translational Psychiatry* **7**, e1165.

Wang Y *et al.* (2017*b*) Altered cerebellar functional connectivity in remitted bipolar disorder: a resting-state functional magnetic resonance imaging study. *Australian & New Zealand Journal of Psychiatry*. doi: 10.1177/0004867417745996.

Wise T *et al.* (2016) Voxel-Based meta-analytical evidence of structural disconnectivity in major depression and bipolar disorder. *Biological Psychiatry* **79**, 293–302.

Zalesky A *et al.* (2016) Connectome sensitivity or specificity: which is more important? *Neuroimage* **142**, 407–420.

Zanetti MV *et al.* (2009) State-dependent microstructural white matter changes in bipolar I depression. *European Archives of Psychiatry and Clinical Neuroscience* **259**, 316–328.